Microchimica Acta (2018) 185: 45
https://doi.org/10.1007/s00604-017-2572-x

ORIGINAL PAPER

Voltammetric sandwich immunoassay for *Cronobacter sakazakii* using a screen-printed carbon electrode modified with horseradish peroxidase, reduced graphene oxide, thionine and gold nanoparticles

Fanjun Zhu[1] · Guangying Zhao[1] · Wenchao Dou[1]

Received: 27 September 2017 / Accepted: 9 November 2017 / Published online: 9 December 2017

Abstract

The authors describe a sandwich-type of electrochemical immunoassay for rapid determination of the foodborne pathogen *Cronobacter sakazakii* (*C. sakazakii*). Polyclonal antibody against *C. sakazakii* (*anti-C. sakazakii*) and horseradish peroxidase were immobilized on a nanocomposite consisting of reduced graphene oxide, thionine and gold nanoparticles (AuNPs) that was placed on a screen-printed carbon electrode (SPCE). Thionine acts as an electron mediator which also shortens the electron transfer pathway from the conjugated HRP to the electrode surface and amplifies the electrochemical signal. The AuNPs, in turn, improve the electron transfer rate and increase the surface area for capturing antibody. The morphologies of the electrodes were characterized by means of field emission scanning electron microscopy. The electrochemical performance of the immunoassay was evaluated by cyclic voltammetry and differential pulse voltammetry. Under optimal experimental conditions, the electrochemical immunoassay, best operated at a woking potential of −0.18 V (vs. Ag/AgCl) and scan rate of 20 mV/s has a linear response that covers the 8.8×10^4 to 8.8×10^8 CFU·mL^{-1} *C. sakazakii* concentration range, with a 1.0×10^4 CFU·mL^{-1} detection limit (at an S/N ratio of 3). The assay was applied to the detemination of *C. sakazakii* in spiked infant milk powder and gave recoveries ranging from 92.0 to 105.7%.

Keywords Electrochemical immunoassay · Foodborne pathogen · HRP · Nanoparticle-based detection

Introduction

Cronobacter sakazakii (*C. sakazakii*) is an important foodborne pathogen, which can cause life-threatening necrotizing entercolitis, meningitis, and sepsis in neonates and infants [1, 2]. Although the incidence caused by *C. sakazakii* is low, the fatality rates is about 40 to 80% and survivors are often left with severe neurological and developmental disorders [3, 4]. *C. sakazakii* has been found in a variety of dry foods, such as powdered infant formula, skim milk powder, herbal teas, and starches [5]. Therefore, the detection of *C. sakazakii* needs high attention and concentration.

Standard microbiological techniques such as bacteriological and biochemical are sensitive, but these methods require complicated procedure, long analysis time and expensive apparatus. It generally requires 5–7 days to detect this pathogen by conventional culture method. These limitations hinder the rapid and sensitive detection of *C. sakazakii.* Compared with conventional bacteriological methods, biochemical methods such as enzyme-linked immunosorbent assay (ELISA) and real-time Polymerase Chain Reaction (PCR) have been used for the identification of *C. sakazakii.* Although these methods have the advantage of high accuracy, they are expensive apparatus required, complicated in operation and time-consuming [6–8]. Therefore, a rapid and sensitive detection method is still needed for the detection of *C. sakazakii.*

Electrochemical immunoassay, as a promising approach for selective and sensitive analyses, has become an important analytical tool in different fields. [9–13]. So far, different electrochemical immunosensors have been used for the

Electronic supplementary material The online version of this article (https://doi.org/10.1007/s00604-017-2572-x) contains supplementary material, which is available to authorized users.

✉ Wenchao Dou
wdou@zjsu.edu.cn

[1] Food Safety Key Laboratory of Zhejiang Province, College of Food Science and Biotechnology, Zhejiang Gongshang University, Hangzhou 310018, China

determination of foodborne pathogenic bacteria [14–17]. In electrochemical immunoassay methods, signaling amplification and noise reduction are very crucial. In general, they are achieved by using an indicator system that results in the amplification of the measured product [18].

The "mediator-HRP" indicator system has been reported in many immunosensors, which showed that this indicator system had potential advantage. The horseradish peroxidase (HRP) and electron mediator were often simultaneously immobilized on a supporter. The supporter not only refrained from adding electroactive materials in the detection solution, but also shortened the electron transfer pathway of the conjugated HRP to the surface of the supporter. Tang et al. reported an electrochemical immunoassay for aflatoxin B1. In that immunoassay, the prussian blue and HRP were immobilized on multifunctional magnetic beads and nanogold, respectively. The pathway of electron transfer was lengthened and the redox of the HRP-H_2O_2 system was lessened [19]. Similarly Tang and his colleague used thionine (TH) and HRP as indicator system of immunosensors to detect thyroid-stimulating hormone and alpha-fetoprotein. And Tang et al. proved that HRP and TH were simultaneously immobilized on one supporter was better than they were separately coated on two supporters [20, 21]. Wang et al. used mesoporous silica nanoparticles and AuNPs as platform to load TH and HRP labeled antibody, and provided a sensitive detection for procalcitonin [22]. Zhang et al. used carbon nanotubes as supporter to immobilize TH and HRP for detection of carcinoembryonic antigen, with a good linear response range and a low limit of detection of 0.008 ng·mL^{-1} [23]. Yuan et al. used graphene oxide to simultaneously immobilize TH labeled antibody and HRP, their work provided a sensitive immunosensor for the detection of carbohydrate antigen 19–9 [24]. Reduced graphene oxide (rGO) has gained great attention in constructing electrochemical biosensors due to its large specific surface area, great electron transfer properties and good biocompatibility [25].

Herein, we designed a novel sandwich-type electrochemical immunoassay for *C. sakazakii* based on the advantages of the rGO. TH, HRP, antibody and gold nanoparticles (AuNPs) were anchored to the surface of rGO (denoted as rGO-TH-AuNPs-Ab-HRP). And we used rGO-TH-AuNPs-Ab-HRP as traces tag and H_2O_2 as enzyme substrates. Additionally, the AuNPs were used to modify screen-printed carbon electrode (SPCE) by electrodeposition.

Experimental

Bioconjugation of anti-*C. sakazakii* and HRP with rGO-TH-AuNPs

The reagents, apparatus and the preparation process of rGO and rGO-TH-AuNPs are provided in Electronic Supplementary Material. 200 μL (20 μg·mL^{-1}) Anti-*C. sakazakii* was added to the 3 mL 1.0 mg·mL $^{-1}$ rGO-TH-AuNPs composites solution and gently mixed at 4 °C for 12 h. After centrifugation, the rGO-TH-AuNPs-Anti-*C. sakazakii* bioconjugates were incubated with 200 μL HRP (5 mg·mL^{-1}) at 4 °C for 12 h. After centrifuged and washed for several times, this bioconjugates were re-dispersed in 1.5 mL phosphate buffered saline (PBS) (containing 0.1 M KCl) and stored at 4 °C when not in use.

Electrochemical measurements procedure

Electrochemical measurements of the immunoassay toward *C. sakazakii* were carried out through a sandwich-type immunoassay mode. The rGO-TH-AuNPs-Ab-HRP was used as trace tag and H_2O_2 was used as enzyme substrates. The preparation of bacterial antigen and the preperation of electrochemical immunoassay were shown in Electronic Supplementary Material. The electrochemical measurements procedure is depicted as follows: (i) 3 μL different concentrations of *C. sakazakii* were dropped on the immunosensor array for 50 min at 36 ± 1 °C, followed by washing with saline to remove unbounded *C. sakazakii*. (ii) 3 μL rGO-TH-AuNPs-Ab-HRP solution was deposited onto the electrode surface for another 50 min, followed by washing with saline to remove unbounded rGO-TH-AuNPs-Ab-HRP. (iii) The electrode was recorded by differential pulse voltammetry (DPV) from −0.45 to 0 V in working buffer containing 4.0 mM H_2O_2. Electrochemical impedance spectroscopy (EIS) measurements were carried out in the presence of a 5.0 mM $Fe(CN)_6^{3-/4-}$ (1:1) mixture in PB (containing 0.1 M KCl). The alternative voltage was 5 mV and the frequency range was 0.1–100,000 Hz. The preparation of stepwise procedure of the sandwich-type immunoassay is shown in Scheme 1.

Results and discussion

Choice of materials

Gold nanoparticles (AuNPs) has been widely used to enhance the sensitivity of the biodetection schemes due to easy to modify with biomaterials, unique electrochemical properties, high surface-to-volume ratios and its small dimensions. Compared with single AuNPs, rGO combined with AuNPs can load more antibodies and increase the sensitivity of the detection result. However, the rGO and AuNPs were negative charge in aqueous solutions and they will not combine with each other directly. Thionine, which owns two hydrophilic -NH_2 symmetrically distributed on each side, has a planar aromatic structure that allows strong interaction with the surface of graphene sheets through synergistic noncovalent charge-transfer and π-stacking forces [26]. The positive charge of thionine not only prevented the aggregation of noncovalent

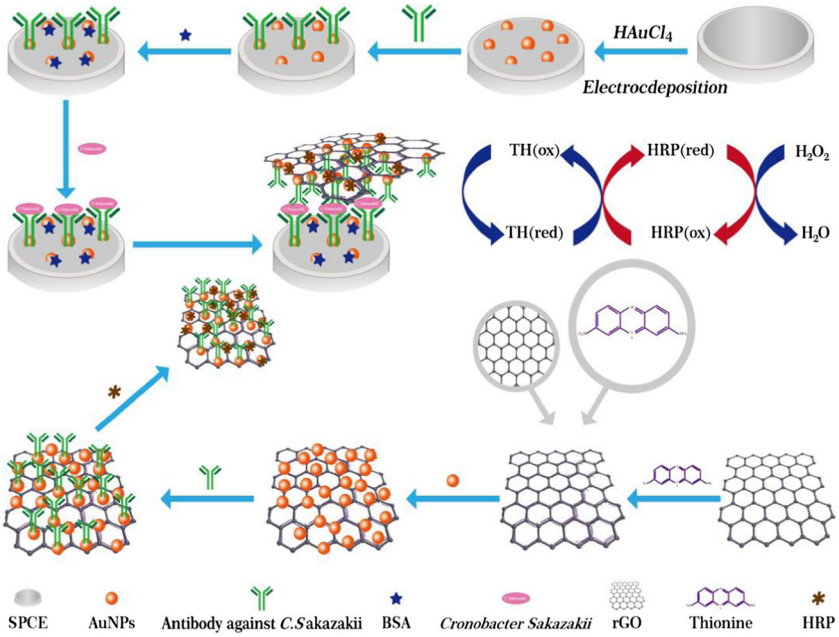

Scheme 1 Fabrication process of rGO-TH-AuNPs nanocomposites and measurement protocol of the electrochemical immunoassay

functionalized rGO but also combine the negatively charged AuNPs absorbed on the surface of rGO. Therefore, we choose rGO-TH-AuNPs as the basic materials in this method.

Characterization of the nanocomposites

The morphologies of rGO and rGO-TH-AuNPs nanocomposites were characterized by field emission scanning electron microscope (FE-SEM) technique. Fig. 1a shows that rGO is irregularly crumpled and wrinkled sheet-like structures, which indicates the rGO has large specific surface area. Fig. 1b shows the morphology of rGO-TH-AuNPs nanocomposites. It shows that a great number of bright dots (AuNPs) are uniformly distributed on the surface of rGO-TH, indicating the formation of rGO-TH-AuNPs nanocomposites. For comparison, we mixed the rGO with the AuNPs without TH molecules. Fig. S1 shows that few AuNPs are anchored on the rGO, it indicates that TH molecules plays an important role in the binding of AuNPs to the rGO. TH not only acts as an electron mediator but also acts as a "bridge" to connect the AuNPs to the rGO. TH is bound to the rGO sheet via π-stacking and synergistic noncovalent charge-transfer. TH can effectively overcome rGO aggregation [27, 28]. The negatively charged AuNPs are absorbed on the surface of rGO-TH because of the interaction between the amine groups in TH and AuNPs together with the electrostatic interaction [29]. The UV-vis absorption spectra, photographs and FTIR spectra of the all kind of nanoparticles and nanocomposites shows in Fig. S2, which illustrates that we have successfully prepared the nanocomposites.

CV and EIS characterization

The preparation of electrochemical immunoassay was provided in Electronic Supplementary Material. Fig. 2a shows the CV of different electrodes in the presence of a 5.0 mM

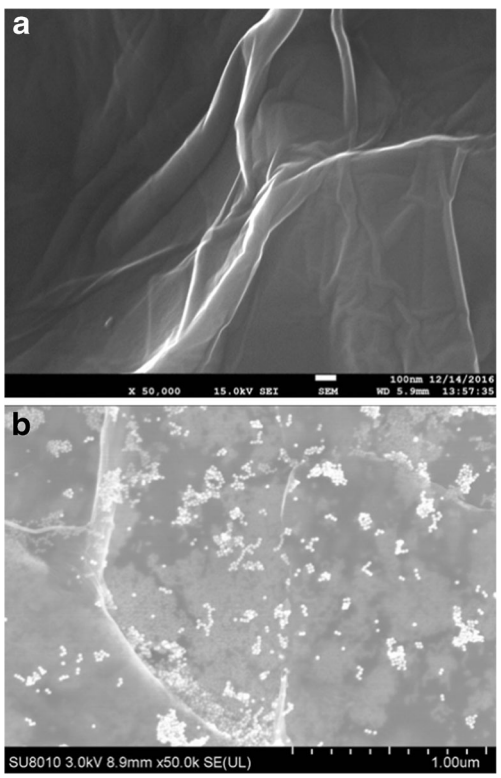

Fig. 1 FE-SEM images of rGO (**a**), rGO-TH-AuNPs nanocomposites (**b**)

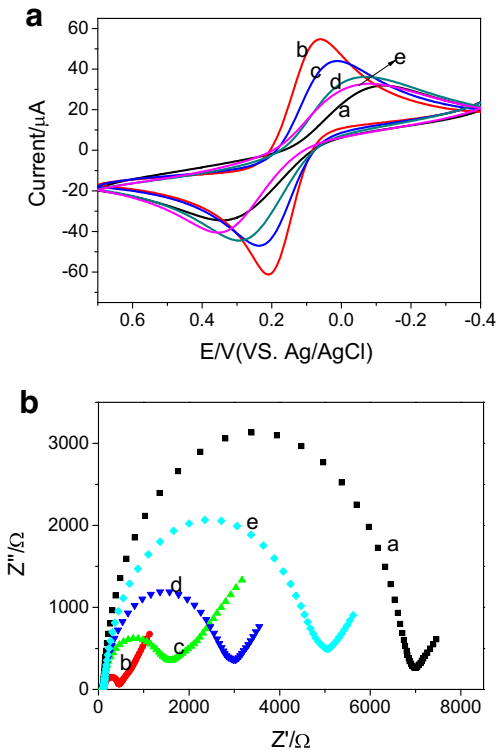

Fig. 2 **a** CV and (**b**) EIS of (a) bare SPCE, (b) AuNPs/SPCE, (c) Ab/AuNPs/SPCE, (d) BSA/Ab/AuNPs/SPCE, (e) *C. sakazakii*/BSA/Ab/AuNPs/SPCE in 5.0 mM $Fe(CN)_6^{3-/4-}$ (1:1) mixture in saline (containing 0.1 M KCl)

$Fe(CN)_6^{3-/4-}$ (1:1) mixture in saline. The redox-label Fe $(CN)_6^{3-/4}$ displays a reversible CV curve at the bare SPCE (curve a), in which appears a pair of well-defined redox peaks. As can be seen from curve b, the cathodic and anodic peak currents are increased obviously after SPCE electrodepositing in $HAuCl_4$. After Anti-*C. sakazakii* self-assembls onto the AuNPs/SPCE (curve c), the peak currents decrease greatly. It indicates that the antibodies are successfully immobilized on the electrode surface. And the immobilized protein acts as the electron communication and mass-transfer blocking layer to insulate the electron transfer of the redox-label $Fe(CN)_6^{3-/4}$ with the electrode. When non-electroactive BSA is used to block nonspecific sites, the peak current further decreases (curve d). The peak current decreases with the *C. sakazakii* immobilization on the electrode (curve e). This can be ascribed to the formation of the antigen-antibody complex which insulated the conductive support and hinder the electron transfer toward the electrode surface.

EIS is employed to further investigate the stepwise modified processes of the electrode. Fig. 2b shows the impedance spectra at different electrodes in $Fe(CN)_6^{3-/4-}$ solution. The semicircle diameter in the impedance spectrum equals to the electron-transfer resistance. As seen from curve a, a big semicircle is observed at the bare SPCE, indicating a high transfer resistance. Subsequently, AuNPs is deposited on the surface of SPCE, the diameter of semicircle is decreased, implying that AuNPs enhance the electron transfer in the electrochemical probe (curve b). When Anti-*C. sakazakii* are self-assembled onto the AuNPs/SPCE, the resistance is increased (curve c). After BSA blocking and subsequent immobilization of *C. sakazakii*, the resistance increases gradually (curve d and e). This is consistent with the fact that the hydrophobic layer of the protein insulates the conductive support and perturbs the interfacial electron transfer. The FE-SEM images of bare SPCE and AuNPs/SPCE are shown in Fig. S3(a) and Fig. S3(b).

CV characteristics of the electrochemical immunoassay

Fig. 3 shows the CV of SPCE, BSA/Ab/AuNPs/SPCE, *C. sakazakii*/Ab/BSA/AuNPs/SPCE and rGO-TH-AuNPs-Ab-HRP/*C. sakazakii*/Ab/BSA/AuNPs/SPCE in pH 5.5 working buffer without or with H_2O_2. No peak is observed at SPCE (curve a), BSA/Ab/AuNPs/SPCE (curve b) and *C. sakazakii* /BSA/Ab/AuNPs/SPCE (curve c). While a pair of stable and well defined redox peaks of TH are obtained using rGO-TH-AuNPs-Ab-HRP/*C. sakazakii*/BSA/Ab/AuNPs/SPCE over the working potential range from −0.5 to 0 V in the working buffer (curve d). Upon addition of 4.0 mM H_2O_2 to the solution, the reduction peak current further increases, the oxidation peak current decreases and the reduction peak potential shifts slightly to a more negative value (curve e). This result indicates an obvious electrocatalytic process, and this electrocatalytic process is mainly derived from the HRP toward the reduction of H_2O_2 with the aid of the TH. It suggests that the HRP as enhancer not only catalyzes the oxidation reaction of TH by H_2O_2, but also blocks nonspecific sites as BSA did.

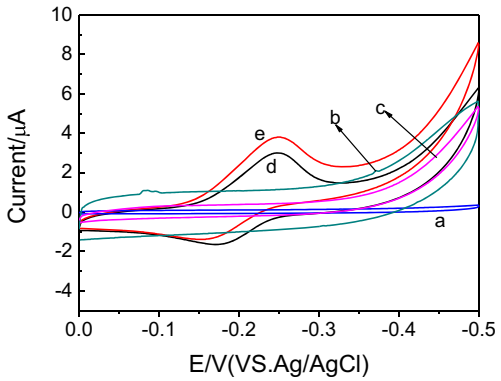

Fig. 3 CV of (**a**) bare SPCE, (**b**) BSA/Ab/AuNPs/SPCE, (**c**) *C. sakazakii*/BSA/Ab/AuNPs/SPCE, and the *C. sakazakii*/BSA/Ab/AuNPs/SPCE after incubation with rGO-TH-AuNPs-Ab-HRP in pH 5.5 working buffer without (**d**) and with (**e**) 4.0 mM H_2O_2 at scan rate of 100 mV s^{-1}

Comparison of electrochemical responses using various signal tags

To highlight the merits of "TH-HRP" indicator system in this immunoassay, we prepared two types of trace tags, i.e. rGO-TH-AuNPs-Ab-HRP and rGO-AuNPs-Ab-HRP (rGO-AuNPs labeled Ab and HRP without TH). They were both used for determination of *C. sakazakii* on the BSA/Ab/AuNPs/SPCE with the same assay format (note: when using rGO-AuNPs, 1 mM TH was directly added into pH 5.5 working buffer containing 4.0 mM H_2O_2). During this process, the conjugated *C. sakazakii* on the BSA/Ab/AuNPs/SPCE was almost the same for each concentration, and thus the produced signal mainly derived from the HRP. Fig. 4 displays the comparison of current responses of the electrochemical immunoassay by using various signal tags. It shows that the use of rGO-TH-AuNPs nanocomposite results in a larger current change than that of the rGO-AuNPs nanocomposite. The reason might be attributed to the following issues [20]: (i) TH molecules acts as a "brige" to connect AuNPs to rGO, which shortened the electron transfer pathway of the conjugated HRP on the surface of rGO-TH-AuNPs nanocomposite. (ii) The exits of TH molecules makes more AuNPs absorbe on the rGO. The rGO-TH-AuNPs nanocomposite exhibites a larger surface coverage for the immobilization of Anti-*C. sakazakii* and HRP than that of rGO-AuNPs nanocomposites. Hence, the high-content HRP molecules on the rGO-TH-AuNPs nanocomposite exhibits high catalytic efficiency toward the reduction of H_2O_2.

Quantificational detection of *C. sakazakii*

Under the optimal conditions (data and figures are given in the Fig. S4 and Fig. S5), the analytical performance of the prepared immunoassay was studied by measuring different concentration *C. sakazakii* with DPV. As shown in Fig. 5, the

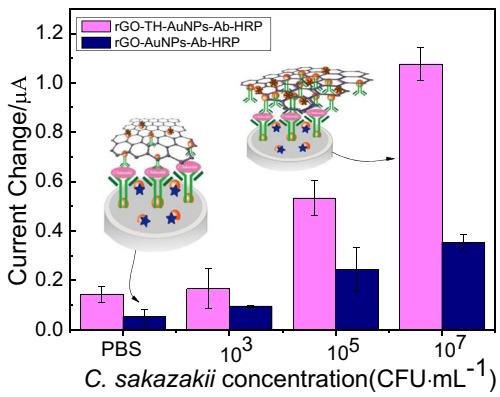

Fig. 4 Comparison of current responses of the BSA/Ab/AuNPs/SPCE toward various *C. sakazakii* concentrations in pH 5.5 working buffer containing 4.0 mM H_2O_2 by using rGO-TH-AuNPs-Ab-HRP (pink) and rGO-AuNPs-Ab-HRP (blue)

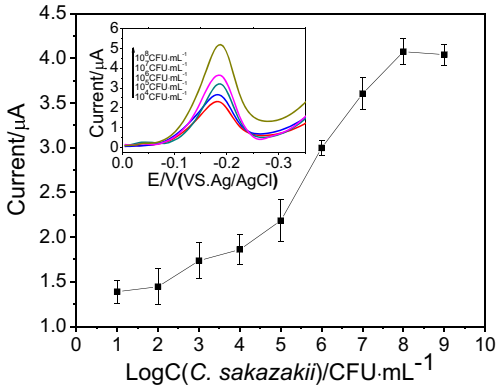

Fig. 5 The current of different concentrations of the *C. sakazakii* in pH 5.5 working buffer containing 4.0 mM H_2O_2 at 20 mV s^{-1}. (Inset: The corresponding DPV curves)

DPV peak currents of the electrochemical immunoassay increases with the increase of *C. sakazakii* concentration. The DPV peak currents and the logarithm values of *C. sakazakii* concentration exhibit a linear relationship in the range of 8.8×10^4–8.8×10^8 CFU·mL^{-1} with a correlation coefficient of 0.987. The linear regression equation is I (μA) = −0.446 + 0.5703lgC (I is the current, μA; C is the concentration of *C. sakazakii*, CFU·mL^{-1}). The limit of detection (LOD) is 1.0×10^4 CFU·mL^{-1} ($S/N = 3$). These results indicate that the immunoassay detection for *C. sakazakii* is reliable and sensitive. The method for the determination of *C. sakazakii* is compared with the previously reported methods in Table 1. It shows that this electrochemical immunoassay has an acceptable analytical performance for the detection of *C. sakazakii*. The electrochemical immunosensor designed by Hu et al. is more sensitive than this work; however, their electrode modification need horseradish peroxidase-labeled antibody and ionic liquids will raise the cost of the experiment. The wide linear range and low LOD can be considered as followed: (i) the excellent electrical conductivity of rGO and AuNPs enhanced the charge transfer; (ii) rGO exhibits a larger surface coverage for the immobilization of Anti-*C. sakazakii* and HRP, and the exit of TH molecules make more AuNPs absorbed on the rGO, (iii) rGO-TH-AuNPs-Ab-HRP as trace tag simultaneously contains the bioactive enzyme (HRP) and electron mediator (TH). rGO-TH-AuNPs nanocomposite not only refrain from adding electroactive materials in the detection solution, but also shorten the electron transfer pathway of the conjugated HRP; (iv) the electrodeposition of AuNPs in the SPCE increases the immobilization amount of antibodies and improve the electronic transmission rate.

Specificity, reproducibility and stability of the immunoassay

The specificity of the electrochemical immunoassay was also monitored toward other foodborne pathogens, such as

Table 1 Comparison of the detection range and LOD of different assays for detection of *C. sakazakii*

Material/method used	Detection range (CFU·mL^{-1})	LOD (CFU·mL^{-1})	Reference
Label-free aptasensing platform	7.1×10^3–7.1×10^7	7.1×10^3	[30]
Sandwich ELISA	2.0×10^4–1.2×10^7	2.0×10^4	[31]
Real-time PCR	10^3–10^9	1.2×10^3	[32]
reduced graphene oxide–gold nanoparticle/ ionic liquid	10^3–10^9	1.19×10^2	[33]
on-chip RPA (recombinase polymerase amplification)	not mentioned	$<1.0 \times 10^2$	[34]
MoS2-Ns aptamer based assay	Digital "Yes or No"kind	10	[35]
Surface Enhanced Raman Spectroscopy	Eight foodborne pathogens	$<1.69 \times 10^2$	[36]
reduced graphene oxide-thionine-gold nanoparticles	8.8×10^4–8.8×10^8	1.0×10^4	This work

C. freundii, *S. aureus*, *B. cereus*, *E. coli*. All of the bacteria solution concentrations were 10^7 CFU·mL^{-1} and saline was used as a blank control. Fig. 6 shows that the peak current is from *C. sakazakii* is much higher than that from the other foodborne pathogens and saline. The results demonstrate that the immunoassay can be used to detect *C. sakazakii* from other foodborne pathogens, indicating good specificity of the electrochemical immunoassay.

To evaluate the reproducibility of the immunoassay, a series of five electrodes were prepared for detecting 8.8×10^7 CFU·mL^{-1} *C. sakazakii*. The relative standard deviation (RSD) of the measurements for the five electrodes was 9.3%, suggesting the reproducibility of the immunoassay is good. Additionally, the stability of the immunoassay was also examined. When the material was stored at 4 °C, it can be seen that 93.3% of the initial response remained after one week and 86.8% of the initial response remained after 30 days, which indicates that the immunoassay had acceptable stability.

Evaluation of *C. sakazakii* in real sample

In order to evaluate the feasibility of the electrochemical immunoassay, recovery experiments were performed by standard addition methods in infant milk powder. A series of milk samples were bought from a market in Hangzhou (Zhejiang, China), and the milk samples were tested for *C. sakazakii* by standard culture method of *C. sakazakii*. And all of milk samples were not affected by *C. sakazakii.* 1.0 mg of infant milk powder was dispersed in 5 mL saline, and then spiked with desired concentrations of 8.8×10^5, 8.8×10^6, 8.8×10^7, 8.8×10^8 CFU·mL^{-1} *C. sakazakii*, respectively, all of which were certified by flat counting method. After that, the samples were determined by the method. As can be seen from Table S1, the recoveries (from 92.0% to 105.7%) are acceptable, but the RSD is relatively high, the reason is ascribed to the fat and protein may influence the detection of *C. sakazakii* in real sample. And the electrochemical immunoassay need to be improved when it is applied in real sample.

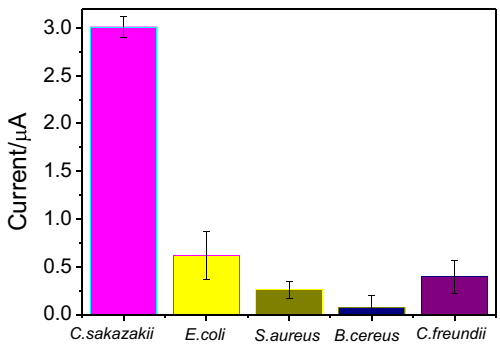

Fig. 6 Specificity of the immunoassay toward: *C. sakazakii*, *E. coli*, *S. aureus*, *B. cereus*, *C. freundii* (from left to right with the same concentration)

Conclusions

In summary, this contribution describes a sandwich type electrochemical immunoassay for the detection of *C. sakazakii* using Anti-*C. sakazakii* and HRP modified rGO-TH-AuNPs nanocomposites as signal amplifying probe. The immunoassay provides a rapid and sensitive detection for *C. sakazakii*, which exhibited acceptable specificity, reproducibility and stability. However, the electrochemical immunoassay needs to be improved when it is applied in real sample because of the relatively instability and not very good recovery. This technique may be useful for future applications in public and food safety.

Acknowledgements This work was financially supported by a grant from National Natural Science Foundation of Zhejiang Province (LY17C200003), the Food and Engineering most important discipline of Zhejiang province (2017SIAR210, JYTSP20141062), Zhejiang public Innovation Platform Analysis and testing project (2015C37023).

Compliance with ethical standards The author(s) declare that they have no competing interests.

Animal studies This article does not contain any studies with animals performed by any of the authors.

Informed consent Informed consent was obtained from all individual participants included in the study.

References

1. Xu X, Li C, Wu Q, Zhang J, Huang J, Yang G (2015) Prevalence, molecular characterization, and antibiotic susceptibility of Cronobacter spp. in Chinese ready-to-eat foods. Int J Food Microbiol 204:17–23
2. Jason J (2012) Prevention of invasive Cronobacter infections in young infants fed powdered infant formulas. Pediatrics 130(5): 1076–1084
3. Bowen AB, Braden CR (2006) Invasive Enterobacter sakazakii disease in infants. Emerg Infect Dis 12(8):1185–1189
4. Friedemann M (2009) Epidemiology of invasive neonatal Cronobacter (Enterobacter sakazakii) infections. Eur J Clin Microbiol Infect Dis 28(11):1297–1304
5. Joseph S, Cetinkaya E, Drahovska H, Levican A, Figueras MJ, Forsythe SJ (2012) Cronobacter condimenti sp. nov., isolated from spiced meat, and Cronobacter universalis sp. nov., a species designation for Cronobacter sp. genomospecies 1, recovered from a leg infection, water and food ingredients. International journal of systematic & evolutionary. Microbiology 62(Pt 6):1277
6. Fricker-Feer C, Cernela N, Bolzan S, Lehner A, Stephan R (2011) Evaluation of three commercially available real-time PCR based systems for detection of Cronobacter species. Int J Food Microbiol 146(2):200
7. Hyeon JY, Park C, Choi IS, Holt PS, Seo KH (2010) Development of multiplex real-time PCR with internal amplification control for simultaneous detection of salmonella and Cronobacter in powdered infant formula. Int J Food Microbiol 144(1):177–181
8. Scharinger EJ, Dietrich R, Kleinsteuber I, Märtlbauer E, Schauer K (2016) Simultaneous rapid detection and serotyping of Cronobacter sakazakii serotypes O1, O2 and O3 using specific monoclonal antibodies. Appl Environ Microbiol 82(8):AEM.04016–AEM.04015
9. Yang Y, Liu Q, Liu Y, Cui J, Liu H, Wang P, Li Y, Chen L, Zhao Z, Dong Y (2017) A novel label-free electrochemical immunosensor based on functionalized nitrogen-doped graphene quantum dots for carcinoembryonic antigen detection. Biosens Bioelectron 90:31–38
10. Chang H, Zhang H, Lv J, Zhang B, Wei W, Guo J (2016) Pt NPs and DNAzyme functionalized polymer nanospheres as triple signal amplification strategy for highly sensitive electrochemical immunosensor of tumour marker. Biosens Bioelectron 86:156–163
11. Cai Y, Li H, Du B, Yang M, Li Y, Wu D, Zhao Y, Dai Y, Wei Q (2011) Ultrasensitive electrochemical immunoassay for BRCA1 using BMIM·BF_4-coated SBA-15 as labels and functionalized graphene as enhancer. Biomaterials 32(8):2117–2123
12. Fei J, Dou W, Zhao G (2015) A sandwich electrochemical immunosensor for salmonella pullorum and Salmonella gallinarum based on a screen-printed carbon electrode modified with an ionic liquid and electrodeposited gold nanoparticles. Microchim Acta 182(13):2267–2275
13. Hernandez-Ibanez N, Garcia-Cruz L, Montiel V, Foster CW, Banks CE, Iniesta J (2016) Electrochemical lactate biosensor based upon chitosan/carbon nanotubes modified screen-printed graphite electrodes for the determination of lactate in embryonic cell cultures. Biosens Bioelectron 77:1168–1174. https://doi.org/10.1016/j.bios.2015.11.005
14. Lin YH, Chen SH, Chuang YC, YC L, Shen TY, Chang CA, Lin CS (2008) Disposable amperometric immunosensing strips fabricated by Au nanoparticles-modified screen-printed carbon electrodes for the detection of foodborne pathogen Escherichia coli O157:H7. Biosens Bioelectron 23(12):1832–1837
15. Bekir K, Barhoumi H, Braiek M, Chrouda A, Zine N, Abid N, Maaref A, Bakhrouf A, Ouada HB, Jaffrezic-Renault N (2015) Electrochemical impedance immunosensor for rapid detection of stressed pathogenic Staphylococcus aureus bacteria. Environ Sci Pollut Res 22(20):15796–15803
16. Gayathri CH, Mayuri P, Sankaran K, Kumar AS (2016) An electrochemical immunosensor for efficient detection of uropathogenic E. coli based on thionine dye immobilized chitosan/functionalized-MWCNT modified electrode. Biosens Bioelectron 82:71–77
17. Zhang X, Shen J, Ma H, Jiang Y, Huang C, Han E, Yao B, He Y (2016) Optimized dendrimer-encapsulated gold nanoparticles and enhanced carbon nanotube nanoprobes for amplified electrochemical immunoassay of E. coli in dairy product based on enzymatically induced deposition of polyaniline. Biosens Bioelectron 80:666
18. Tang D, Su B, Tang J, Ren J, Chen G (2010) Nanoparticle-based Sandwich Electrochemical Immunoassay for Carbohydrate Antigen 125 with Signal Enhancement Using Enzyme-Coated Nanometer-Sized Enzyme-Doped Silica Beads. Anal Chem 82(4): 1527–1534
19. Tang D, Zhong Z, Niessner R, Knopp D (2009) Multifunctional magnetic bead-based electrochemical immunoassay for the detection of aflatoxin B1 in food. Analyst 134(8):1554–1560
20. Zhang B, Tang D, Liu B, Cui Y, Chen H, Chen G (2012) Nanogold-functionalized magnetic beads with redox activity for sensitive electrochemical immunoassay of thyroid-stimulating hormone. Anal Chim Acta 711(2):17
21. Zeng L, Li Q, Tang D, Chen G, Wei M (2012) Metal platinum-wrapped mesoporous carbon for sensitive electrochemical immunosensing based on cyclodextrin functionalized graphene nanosheets. Electrochim Acta 68(5):158–165
22. Fang YS, Wang HY, Wang LS, Wang JF (2014) Electrochemical immunoassay for procalcitonin antigen detection based on signal amplification strategy of multiple nanocomposites. Biosens Bioelectron 51(1):310–316
23. Feng D, Li L, Fang X, Han X, Zhang Y (2014) Dual signal amplification of horseradish peroxidase functionalized nanocomposite as trace label for the electrochemical detection of carcinoembryonic antigen. Electrochim Acta 127:334–341
24. Yang F, Yang Z, Zhuo Y, Chai Y, Yuan R (2014) Ultrasensitive electrochemical immunosensor for carbohydrate antigen 19-9 using Au/porous graphene nanocomposites as platform and Au@Pd core/shell bimetallic functionalized graphene nanocomposites as signal enhancers. Biosens Bioelectron 66:356
25. Veerapandian M, Hunter R, Neethirajan S (2016) Dual immunosensor based on methylene blue-electroadsorbed graphene oxide for rapid detection of the influenza a virus antigen. Talanta 155:250–257
26. Cao C, Zhai W, Lu D, Zhang H, Zheng W (2011) A facile method to prepare stable noncovalent functionalized graphene solution by using thionine. Mater Res Bull 46(4):583–587
27. Chen C, Zhai W, Lu D, Zhang H, Zheng W (2011) A facile method to prepare stable noncovalent functionalized graphene solution by using thionine. Mater Res Bull 46(4):583–587. https://doi.org/10.1016/j.materresbull.2010.12.024
28. Feng D, Li L, Han X, Fang X, Li X, Zhang Y (2014) Simultaneous electrochemical detection of multiple tumor markers using functionalized graphene nanocomposites as non-enzymatic labels. Sensors Actuators B Chem 201:360–368. https://doi.org/10.1016/j.snb.2014.05.015
29. Kong FY, MT X, JJ X, Chen HY (2011) A novel lable-free electrochemical immunosensor for carcinoembryonic antigen based on gold nanoparticles-thionine-reduced graphene oxide nanocomposite film modified glassy carbon electrode. Talanta 85(5):2620–2625. https://doi.org/10.1016/j.talanta.2011.08.028
30. Kim HS, Kim YJ, Chon JW, Kim DH, Yim JH, Kim H, Seo KH (2017) Two-stage label-free aptasensing platform for rapid

detection of Cronobacter sakazakii in powdered infant formula. Sensors Actuators B Chem 239:94–99

31. Xu X, Zhang Y, Shi M, Sheng W, Du X, Yuan M, Wang S (2014) Two novel analytical methods based on polyclonal and monoclonal antibodies for the rapid detection of Cronobacter spp.: development and application in powdered infant formula. LWT Food Sci Technol 56(2):335–340
32. Wang X, Zhu C, Xu X, Zhou G (2012) Real-time PCR with internal amplification control for the detection of Cronobacter spp. (Enterobacter sakazakii) in food samples. Food Control 25(1): 144–149
33. Hu X, Dou W, Zhao G (2015) Electrochemical immunosensor for Enterobacter sakazakii detection based on electrochemically reduced graphene oxide–gold nanoparticle/ionic liquid modified electrode. J Electroanal Chem 756(2):43–48
34. Kersting S, Rausch V, Bier FF, Nickisch-Rosenegk MV (2014) Multiplex isothermal solid-phase recombinase polymerase amplification for the specific and fast DNA-based detection of three bacterial pathogens. Microchim Acta 181(13):1715–1723
35. Singh P, Gupta R, Sinha M, Kumar R, Bhalla V (2016) MoS 2 based digital response platform for aptamer based fluorescent detection of pathogens. Microchim Acta 183(4):1501–1506
36. Mungroo NA, Oliveira G, Neethirajan S (2016) SERS based point-of-care detection of food-borne pathogens. Microchim Acta 183(2): 697–707